JMM

An efficient numerical approach for singularly perturbed parabolic convection-diffusion problems with large time-lag

Naol Tufa Negero[†][*]**, Gemechis File Duressa**[‡]

[†]*Department of Mathematics, College of Natural Science, Wollega University, Nekemte, Ethiopia*
[‡]*Department of Mathematics, College of Natural Science, Jimma University, Jimma, Ethiopia*
Email(s): natitfa@gmail.com, gammeef@gmail.com

Abstract. In this paper, an efficient finite difference method is presented for solving singularly perturbed linear second order parabolic problems with large time lag. The comparable numerical model is related to automatically controlled system with spatial diffusion of reactants in the processes. This study focuses on the formation of boundary layer behavior or oscillatory behaviors due to the presence of delay parameters and perturbation parameter. The numerical scheme comprising an exponentially fitted spline based difference scheme on a uniform mesh supported by Crank-Nicolson Method is constructed. It is found that the present method converges with second order accurate in both temporal and spatial variables. The convergence analysis and running time of the program with varied grid sizes are then used to do the efficiency analysis. The proposed scheme accuracy and efficiency are also demonstrated through numerical experiments.

Keywords: Singular perturbation, parabolic convection-diffusion, large time delay, exponentially fitted method, parameter uniform convergence.
AMS Subject Classification 2010: 65M06, 65M12, 65M15.

1 Introduction

In many practical applications larger systems of ordinary or partial differential equations can be quite good at approximating observed behavior, but the difficulties with those cases come from the involvement of various parameters. To deal with such difficulties several approaches have been developed in [11, 13]. Nowadays delay differential equations are used to describe many physical phenomena of interest in science and engineering and its numerical approximation still on rapid growth (see e.g., [2, 5, 8, 12, 14, 21]). Depending on the response of the system many applications can be delayed in a more complicated way.

There are many examples where time delay and spatial diffusion enter control systems [6, 17–19]. Numerous models of delay parabolic partial differential equations can be found in [22]. Simplified mathematical description of the overall control system in the form of singularly perturbed delay parabolic partial differential equation was given in the paper [1]. In recent years there has been a developmental activity in the numerical study of singularly perturbed time delay parabolic partial differential equations of convection-diffusion type. Numerical schemes such as, uniformly convergent hybrid numerical scheme by Das and Natesan [3], second-order uniformly convergent numerical method by Das and Natesan [4], ε-uniformly convergent numerical scheme by Gowrisankar and Natesan [7], parameter-uniform numerical scheme by Kumar and Kumari [9], and new stable finite difference (NSFD) scheme by Podila and Kumar [16]. To our knowledge, no exponentially fitted approach based on spline has yet yielded results in approximating the solution of singularly perturbed parabolic partial differential equations with large-time delay. This partially motivated our interest to enhance suitable numerical approach for numerical strategies to deal with the oscillatory nature of the solutions when the perturbation parameter ε will become very small whose accuracy does not depend on the parameter value ε.

The main aim of this article is to construct and analyze the exponentially fitted spline based technique to provide better approximate numerical solution for the singularly perturbed parabolic partial differential equations with large-time lag. Since the solution of the singularly perturbed parabolic partial differential equations with large-time lag exhibits boundary layer, we discretize the domain by uniform mesh in both time and spatial directions. In this method the time derivative is approximated by Crank-Nicolson method, and the spatial derivatives are approximated by the exponentially fitted spline-based approach. The advantage of this method is that, it is not required to have any restriction on the mesh generation.

2   Continuous problem

We consider the following initial-boundary value problems (IBVPs) for a singularly perturbed time-delay parabolic convection-diffusion equation

$$\begin{aligned}
\pounds_\varepsilon u \equiv -\varepsilon u_{xx}(x,t) + a(x,t)u_x(x,t) + b(x,t)u(x,t) \\
= -c(x,t)u(x,t-\tau) + f(x,t) - \frac{\partial u}{\partial t}, \quad (x,t) \in D,
\end{aligned} \tag{1}$$

with the boundary conditions

$$\begin{cases}
u(0,t) = \phi_l(t), & \Gamma_l = \{(0,t) : 0 \le t \le T\}, \\
u(1,t) = \phi_r(t), & \Gamma_r = \{(1,t) : 0 \le t \le T\},
\end{cases} \tag{2}$$

and the interval initial condition

$$u(x,t) = \phi_b(x,t), \quad (x,t) \in \Gamma_b = [0,1] \times [-\tau,0]. \tag{3}$$

Here $\Omega_x = (0,1)$, $D = \Omega_x \times (0,T]$, $\Gamma = \Gamma_l \cup \Gamma_b \cup \Gamma_r$, where Γ_l and Γ_r are the left and the right side of the rectangular domain D corresponding to $x = 0$ and $x = 1$, respectively and $\Gamma_b = [0,1] \times [-\tau,0]$, $0 < \varepsilon \ll 1$ is a singular perturbation parameter and $\tau > 0$ represents the delay parameter and the data $a(x,t), b(x,t), f(x,t)$ on $\overline{D}$ and $\phi_b(x,t), \phi_l(t), \phi_r(t)$ on Γ are sufficiently smooth, bounded functions that satisfy

$$a(x,t) \ge \alpha > 0, \quad b(x,t) \ge \beta > 0, \quad (x,t) \in \overline{D}.$$

2.1 Properties of continuous solution

The existence and uniqueness of the solution for the model problem Eqs. (1)-(3) can be guaranteed by the sufficient smoothness of $\phi_l(t), \phi_b(x,t)$ and $\phi_r(t)$ along with appropriate compatibility conditions at the corner points $(0,0), (1,0), (0,-\tau)$ and $(1,-\tau)$, and delay terms as stated below:

$$\begin{cases} \phi_b(0,0) = \phi_l(0), \\ \phi_b(1,0) = \phi_r(0), \end{cases} \tag{4}$$

and

$$\begin{cases} \frac{\partial \phi_l(0)}{\partial t} - \varepsilon \frac{\partial^2 \phi_b(0,0)}{\partial x^2} + a(0,0)\frac{\partial \phi_b(0,0)}{\partial x} + b(0,0)\phi_b(0,0) = -c(0,0)\phi_b(0,-\tau) + f(0,0), \\ \frac{\partial \phi_r(0)}{\partial t} - \varepsilon \frac{\partial^2 \phi_b(1,0)}{\partial x^2} + a(1,0)\frac{\partial \phi_b(1,0)}{\partial x} + b(1,0)\phi_b(1,0) = -c(1,0)\phi_b(0,-\tau) + f(1,0). \end{cases} \tag{5}$$

Setting $\varepsilon = 0$, the reduced problem corresponding to Eqs. (1)-(3) is given by

$$\frac{\partial u_0}{\partial t} + a(x,t)u_0(x,t) = -b(x,t)u_0(x,t-\tau) + f(x,t), \quad (x,t) \in D, \tag{6}$$

with the boundary conditions

$$\begin{cases} u_0(0,t) = \phi_l(t), & \Gamma_l = \{(0,t) : 0 \le t \le T\}, \\ u_0(1,t) \ne \phi_r(t), & \Gamma_r = \{(1,t) : 0 \le t \le T\}, \end{cases} \tag{7}$$

and the interval initial condition

$$u_0(x,t) = \phi_b(x,t), \quad (x,t) \in (x,t) \in \Gamma_b = [0,1] \times [-\tau,0]. \tag{8}$$

Therefore, it is clear that the solution of Eqs. (1)-(3) has a boundary layers on Γ_r. In this study, our aim is to obtain and examine the approximate solution to observe the effect of the parameter ε on the boundary layer.

Lemma 1 (Continuous maximum principle). *Assume that the function $\eta(x,t) \in C^2(D) \cap C^0(\bar{D})$. Suppose that $\pounds_\varepsilon \eta(x,t) \ge 0$ for all $(x,t) \in D$ and $\eta(x,t) \ge 0$ for all $(x,t) \in \Gamma$. Then $\eta(x,t) \ge 0$ for all $(x,t) \in \bar{D}$.*

Proof. Let $(\xi,\vartheta) \in D$ be such that $\eta(\xi,\vartheta) = \min_{(x,t)\in\bar{D}} \eta(x,t)$ and suppose $\eta(\xi,\vartheta) < 0$. It is clear that $(\xi,\vartheta) \notin \Gamma$ as $\eta(x,t) \ge 0$ on Γ. Since at the point (ξ,ϑ) the function η attains minimum, then, we have $\eta_x(\xi,\vartheta) = \eta_t(\xi,\vartheta) = 0$ and $\eta_{xx}(\xi,\vartheta) \ge 0$ at point (ξ,ϑ). Using $\pounds_\varepsilon$ on $\eta(x,t)$, from Eq. (2) we have

$$\pounds_\varepsilon \eta(\xi,\vartheta) = \eta_t(\xi,\vartheta) - \varepsilon \eta_{xx}(\xi,\vartheta) + a(\xi,\vartheta)u_x(\xi,\vartheta) + b(\xi,\vartheta)\eta(\xi,\vartheta),$$

since $\eta_{xx}(\xi,\vartheta) > 0, \eta_t(\xi,\vartheta) = \eta_x(\xi,\vartheta) = 0$ we get $\pounds_\varepsilon \eta(\xi,\vartheta) < 0$, which contradicts the given assumption as $\pounds_\varepsilon \eta(x,t) \ge 0$ in D. Hence, we have $\eta(x,t) \ge 0$ for all $(x,t) \in \bar{D}$. $\qquad\square$

Using maximum principle given in Lemma 1 and compatibility conditions in Eqs. (4) and (5) we can say that there exists a constant C independent of ε such that for all $(x,t) \in \overline{D}$ we have the following Lemmas.

Lemma 2. *The solution $u(x,t)$ of the continuous problem in Eqs. (1)-(3) satisfies the following estimation:*

$$|u(x,t) - \phi_b(x,0)| \le Ct.$$

Proof. For the proof reader can refer to Das and Natesan [3].   □

Lemma 3. *The bound on the solution $u(x,t)$ of the continuous problem in Eqs. (1)-(3) satisfy the following bound:*

$$|u(x,t)| \le C, \quad (x,t) \in \bar{D}.$$

Proof. From Lemma 2, we have

$$|u(x,t)| - |\phi_b(x,0)| \le |u(x,t) - \phi_b(x,0)| \le Ct.$$

Hence,

$$u(x,t) \le Ct + \phi_b(x,0), \quad \forall(x,t) \in \bar{D}.$$

Since $t \in (0,T]$, so it is bounded and $\phi_b(x,0) \in C^2(\bar{D})$. Therefore, $Ct + \phi_b(x,0)$ is bounded by some constant C and hence $|u(x,t)| \le C$, $(x,t) \in \bar{D}$.   □

Lemma 4. *[3] The bounds on the derivatives of the exact solution $u(x,t)$ of the model problems in Eqs. (1)-(3) satisfies*

$$\left| \frac{\partial^{i+j} u}{\partial x^i \partial t^j} \right| \le C \left(1 + \varepsilon^{-i} \exp\left(-\alpha\left(1-x\right)/\varepsilon \right) \right), \forall(x,t) \in \bar{D},$$

where i and j are non-negative integers such that $0 \le i+j \le 5$.

3   Numerical schemes

3.1   The time semidiscretization

In this section, a numerical scheme which works nicely when delay parameter τ are larger than perturbation parameter ε. Now, for the delay term $u(x, t - \tau)$ we construct a special type of mesh so that the terms containing the delay parameter τ lie on the mesh points after discretization. This can be done as first dividing the given interval $[-\tau, 0]$ into s equal parts with spacing $\Delta t = \tau/s$ and use the same spacing for the interval $[0,T]$. Thus, the mesh for $[0,T]$ is defined as

$$\bar{\Omega}_t^M = \{t_n = n\Delta t, \ n = 0, 1, \ldots, T/\Delta t\},$$

where $M = T/\Delta t$ is the total number of mesh elements in the temporal direction in the interval $[0,T]$ and so the mesh in the interval $[-\tau, T]$ is defined as

$$\bar{\Omega}_\Gamma^s = \{t_n = n\Delta t, \ n = 0, 1, ..., s, \ \Delta t = \tau/s\},$$

where $\bar{\Omega}_\Gamma^s$ and $\bar{\Omega}^M$ are the uniform meshes discretized with step size Δt such that s and M mesh elements are used on $[-\tau, 0]$ and $[0,T]$, respectively. Then $u(x, t - \tau)$ is a known function on $[0, 1] \times [0, \tau]$ and Eqs. (1)-(3) becomes a classical singularly perturbed parabolic partial differential equations, and can

be treated using the known existence theories. Discretization of the time derivative by means of the Crank-Nicolson's method in Eqs. (1)-(3) on $\Omega \times \bar{\Omega}^M$ yields the following,

$$
\begin{cases}
\dfrac{U^{n+1}(x) - U^n(x)}{\Delta t} - \varepsilon (U_{xx})^{n+1/2}(x) + a^{n+1/2}(x)(U_x)^{n+1/2}(x) + b^{n+1/2}(x)U^{n+1/2}(x) \\
\qquad = -c^{n+1/2}(x)U^{n+1/2-s}(x) + f^{n+1/2}(x), \\
U^{n+1}(0) = \phi_l(t_{n+1}), \quad 0 \le n \le M, \\
U^{n+1}(1) = \phi_r(t_{n+1}), \quad 0 \le n \le M, \\
U^{n+1}(x) = \phi_b(x, t_{n+1}), \quad x \in \Omega_x, -(s+1) \le n \le -1,
\end{cases}
\tag{9}
$$

where $U^{n+1/2}(x) = \left(U^{n+1}(x) + U^n(x)\right)/2$ and $U^{n+1}(x)$ is an approximate solution of $u(x, t_{n+1})$ at $(n + 1)^{th}$ time level.

Using differential operator and discretization process of Eq. (9) yields the following semi-discrete method,

$$
\left(I + \dfrac{\Delta t}{2} \pounds_\varepsilon^*\right) U^{n+1}(x) =
\begin{cases}
U(x, t_n) + \dfrac{\Delta t}{2}\left(\hat{\Lambda}^n(x) + \hat{\Lambda}^{n+1}(x) - \pounds_\varepsilon U(x, t_n)\right), \\
\qquad n = 0, 1, \dots, s, \ x \in \Omega_x, \\
U(x, t_n) + \dfrac{\Delta t}{2}\left(\Lambda^n(x) + \Lambda^{n+1}(x) - \pounds_\varepsilon U(x, t_n)\right), \\
\qquad n = s+1, \dots, M-1, \ x \in \Omega_x, \\
U^{n+1}(0) = \phi_l(t_{n+1}), \ U^{n+1}(1) = \phi_r(t_{n+1}), \\
\qquad 0 \le n \le M,
\end{cases}
\tag{10}
$$

where

$$
\begin{aligned}
\hat{\Lambda}^n(x) &= -c(x, t_n)\phi_b(x, t_{n+1})) + f(x, t_n), \\
\Lambda^n(x) &= -c(x, t_n)u(x, t_{n-s})) + f(x, t_n), \\
\pounds_\varepsilon^* U(x, t_{n+1}) &= -\varepsilon u_{xx}(x, t_{n+1}) + a(x, t_{n+1})u_x(x, t_{n+1}) + b(x, t)u(x, t_{n+1}).
\end{aligned}
$$

The semidiscrete operator $\left(I + \frac{\Delta t}{2}\pounds_\varepsilon^*\right)U^{n+1}(x)$ in Eq. (10) satisfies the maximum principle as follows.

Lemma 5 (Semi-discrete maximum principle). *Let* $\Pi^{n+1}(x)$ *be a smooth function such that* $\Pi^{n+1}(0) \ge 0$ *and* $\Pi^{n+1}(1) \ge 0$. *Then* $\pounds_\varepsilon^* \Pi^{n+1}(x) \ge 0$ *for all* $x \in D$, *implies that* $\Pi^{n+1}(x) \ge 0$ *for all* $x \in \bar{D}$.

Proof. Let $(\xi, t_{n+1}) \in \{(x, t_{n+1}) : x \in \bar{D}\}$ be such that $\Pi^{n+1}(\xi) = \min_{(x) \in \bar{D}} \Pi^{n+1}(x)$ and $\Pi^{n+1}(x) < 0$. It is clear that $(\xi, t_{n+1}) \notin \{(0, t_{n+1}), (1, t_{n+1})\}$ as $\Pi^{n+1}(x) \ge 0$ on $\{0, 1\}$. Then, we have $\Pi_x^{n+1}(\xi) = 0$ and $\Pi_{xx}(\xi) \ge 0$ and thus,

$$
\left(I + \frac{\Delta t}{2}\pounds_\varepsilon^*\right) U^{n+1}(\xi) = -\frac{\varepsilon}{2}(\Pi_{xx})^{n+1}(\xi) + \frac{a^{n+1/2}(\xi)}{2}(\Pi_x)^{n+1}(\xi) + \frac{b^{n+1/2}(\xi)}{2}\Pi^{n+1}(\xi)
$$

$$
\le \frac{b^{n+1/2}(\xi)}{2}\Pi^{n+1}(\xi) < 0,
$$

which contradicts our supposition and $\Pi^{n+1}(\xi) \ge 0$. This implies $\Pi^{n+1}(x) \ge 0$ for all $(x) \in \bar{D}$. $\qquad \square$

The local truncation error e_{n+1} of the temporal semi-discretization Eq. (10) is given by $U^n(x) - u(x,t_n)$ where $u(x,t_n)$ and $U^n(x)$ are the exact and approximate solution of the problem in Eqs. (1)-(3). Now we follow the following lemma for the error estimation e_{n+1}.

Lemma 6 (**Local error estimate**). *Suppose that Lemma 4 hold. Then the local error estimation associated to the semi-discretized problem Eq. (10) is given by* $\|e_{n+1}\| \leq C(\Delta t)^3$.

Proof. The proof follows easily from [9].   □

Lemma 7 (**Global error estimate**). *The global error estimation in the temporal direction is given by*

$$\|E_{n+1}\| \leq C(\Delta t)^2,$$

where E_{n+1} is the global error in the temporal direction at $(n+1)th$ time level.

Proof. Using local error estimates given in Lemma 6, the global error estimate at the $(n+1)th$ time step is given by

$$\|E_n\| = \left\|\sum_{k=1}^{n} e_k\right\|, \qquad\qquad \left(n \leq \frac{T}{\Delta t}\right)$$
$$\leq \|e_1\| + \|e_2\| + \cdots + \|e_n\|$$
$$\leq C_0\left((n)\Delta t\right)^2(\Delta t) \qquad \text{(using Lemma 6)}$$
$$\leq C_0 T(\Delta t)^2, \qquad\qquad \text{(since } n(\Delta t) \leq T)$$
$$\leq C(\Delta t)^2, \qquad\qquad C = C_0 T,$$

where C is constant independent of ε and Δt.   □

Using the following Lemma we bound for the derivatives of solution of Eq. (10).

Lemma 8. *[9] The solution $U^n(x)$ of semi-discretized problem in Eq. (10) and its derivatives satisfy*

$$\left|\frac{d^i U^{n+1}(x)}{dx^i}\right| \leq C\left(1 + \varepsilon^{-i} exp\left(-\alpha(1-x)/\varepsilon\right)\right), \forall (x,t) \in \bar{D}, \quad i = 0,1,2,3.$$

3.2   The spatial discretization

In this section we keep the temporal direction as a constant and for the spacial direction we consider a uniform mesh with nodal points x_m on the spatial domain $[0,1]$ such that: $0 = x_0 < x_1 < \cdots < x_N = 1$, $h = x_m - x_{m-1} = 1/N$. Now, if we regard

$$g(t,x,u(x,t),u_x(x,t)) = -c(x,t)u(x,t-\tau) + f(x,t) - a(x,t)u_x(x,t) - b(x,t)u(x,t) - u_t(x,t), \quad (11)$$

then Eq. (1) becomes

$$-\varepsilon u_{xx}(x,t) = g(t,x,u(x,t),u_x(x,t)). \tag{12}$$

Taking the Taylor expansion for first order derivative of $u(t)$, we get the following fourth order approximations:

$$
\begin{cases}
u_x(x_m,t) \approx \dfrac{u_{m+1}(t) - u_{m-1}(t)}{2h}, \\[2mm]
u_x(x_{m+1},t) \approx \dfrac{3u_{m+1}(t) - 4u_m(t) + u_{m-1}(t)}{2h}, \\[2mm]
u_x(x_{m-1},t) \approx \dfrac{-u_{m+1}(t) + 4u_m(t) - 3u_{m-1}(t)}{2h}, \\[2mm]
\hat{u}_x(x_m,t) \approx u_x(x_m,t) - \dfrac{1}{12}\left(\hat{g}_{m+1}(t) - \hat{g}_{m-1}(t)\right),
\end{cases}
\tag{13}
$$

and

$$
-\varepsilon\sigma(\rho)\frac{\delta_x^2 U(t)}{h^2} = \frac{1}{12}\left(\hat{g}_{m+1}(t) + 10\bar{g}_m(t) + \hat{g}_{m-1}(t)\right),
\tag{14}
$$

where

$$
\begin{aligned}
\delta_x^2 U_m(t) &= U_{m-1}(t) - 2U_m(t) + U_{m+1}(t), \\
\bar{g} &= g\left(t, x_m, u(x_m,t), \hat{u}_x(x_m,t)\right), \\
\hat{g}_{m\pm1} &= g\left(t, x_{m\pm1}, u(x_{m\pm1},t), u_x(x_{m\pm1},t)\right),
\end{aligned}
$$

and $\sigma(\rho)$ is an artificial viscosity which is to be determined in the next section.

3.2.1 Computation of the artificial viscosity

Here, the main aim is to determine the value of the introduced artificial viscosity $\sigma(\rho)$. From the theory of singular perturbations described in O'Malley [15] and taking the Taylor's series expansion for $a(x,t)$ about the point '1', and restricting to their first terms, the solution of Eqs. (1)-(3) can be written in form

$$
u(x,t) = u_0(x,t) + (\phi_r - u_0(1,t))\exp\left(-\frac{a(1,t)(1-x)}{\varepsilon}\right) + O(\varepsilon),
\tag{15}
$$

with $u_0(x,t)$ is the solution of the reduced problems in Eqs. (1)-(3) obtained by setting $\varepsilon = 0$. Also from Eq. (15), we obtain

$$
u(mh,t) = u_0(mh,t) + (\phi_r - u_0(1,t))\exp\left(-\frac{a(1,t)}{\varepsilon}(1-mh)\right).
$$

Therefore,

$$
\lim_{h\to 0} u(mh,t) = u_0(0,t) + (\phi_r - u_0(1,t))\exp\left(-a(1,t)\left(\frac{1}{\varepsilon} - m\rho\right)\right),
\tag{16}
$$

where $\rho = h/\varepsilon$. Now, multiplying Eq. (14) by h and evaluating the limit as $h \to 0$ gives:

$$
\lim_{h\to 0}\left[\frac{\sigma(\rho)}{\rho}\left(u_{m+1}(t) - 2u_m(t) + u_{m-1}(t)\right)\right] + \frac{1}{2}a(mh,t)\left(u_{m+1}(t) - u_{m-1}(t)\right) = 0.
\tag{17}
$$

Using Eq. (16) into Eq. (17) and taking $a(x,t) = a = $ constant, $b(x,t) = b = $ constant and on simplifying, we get

$$\sigma(\rho) = \frac{\rho a(1,t)}{2}\coth\left(\frac{\rho a(1,t)}{2}\right).$$

So for equation with a variable coefficient we define the artificial viscosity for the parameter ε as

$$\sigma(\rho) = \frac{\rho a(x_m,t)}{2}\coth\left(\frac{\rho a(x_m,t)}{2}\right).$$

3.3 Fully discrete scheme

In this section, we combine the obtained schemes in Eqs. (10) and (14). Now, introducing the artificial viscosity $\sigma_1(\rho)$ and $\sigma_2(\rho)$ at both $(m,n+1)$th and (m,n)th level respectively, we arrive at the following difference scheme:

$$
\begin{cases}
\left(q_m^- + \frac{\Delta t}{2}r_m^-\right)U_{m-1}^{n+1} + \left(q_m^c + \frac{\Delta t}{2}r_m^c\right)U_m^{n+1} + \left(q_m^+ + \frac{\Delta t}{2}r_m^+\right)U_{m+1}^{n+1} = \\[2mm]
\left(q_m^- - \frac{\Delta t}{2}\hat{r}_m^-\right)U_{m-1}^n + \left(q_m^c - \frac{\Delta t}{2}\hat{r}_m^c\right)U_m^n + \left(q_m^+ - \frac{\Delta t}{2}\hat{r}_m^+\right)U_{m+1}^n \\[2mm]
-\frac{\Delta t}{2}q_m^-\left(c_{m-1}^{n+1}H_{m-1}^{n+1} + c_{m-1}^n H_{m-1}^n\right) - \frac{\Delta t}{2}q_m^c\left(c_m^{n+1}H_m^{n+1} + c_m^n H_m^n\right) - \\[2mm]
\frac{\Delta t}{2}q_m^+\left(c_{m+1}^{n+1}H_{m+1}^{n+1} + c_{m+1}^n H_{m+1}^n\right) + \frac{\Delta t}{2}q_m^-\left(f_{m-1}^{n+1} + f_{m-1}^n\right) + \\[2mm]
\frac{\Delta t}{2}q_m^c\left(f_m^{n+1} + f_m^n\right) + \frac{\Delta t}{2}q_m^+\left(f_{m+1}^{n+1} + f_{m+1}^n\right),
\end{cases}
\tag{18}
$$

and the coefficients are given by

$$
\begin{cases}
r_m^- = -\varepsilon\sigma_1(\rho) - \frac{3}{2}\eta_1 ha_{m-1}^{n+1} - \eta_2 ha_m^{n+1} + \frac{1}{2}\eta_1 ha_{m+1}^{n+1} + \eta_1 h^2 b_{m-1}^{n+1} \\[2mm]
\qquad - \eta_1 h^2\left(\frac{h}{2}a_m^{n+1}b_{m-1}^{n+1} - \frac{1}{4}a_m^{n+1}\left(a_{m+1}^{n+1} + 3a_{m-1}^{n+1}\right)\right), \\[2mm]
r_m^c = 2\varepsilon\sigma_1(\rho) + 2\eta_1 ha_{m-1}^{n+1} - 2\eta_1 ha_{m+1}^{n+1} + 2h^2\eta_2 b_m^{n+1} - \eta_1 h^2 a_m^{n+1}\left(a_{m+1}^{n+1} + a_{m-1}^{n+1}\right), \\[2mm]
r_m^+ = -\varepsilon\sigma_1(\rho) - \frac{1}{2}\eta_1 ha_{m-1}^{n+1} + \eta_2 ha_m^{n+1} + \frac{3}{2}\eta_1 ha_{m+1}^{n+1} + \eta_1 h^2 b_{m+1}^{n+1} \\[2mm]
\qquad + \eta_1 h^2\left(\frac{h}{2}a_m^{n+1}b_{m+1}^{n+1} + \frac{1}{4}a_m^{n+1}\left(3a_{m+1}^{n+1} + a_{m-1}^{n+1}\right)\right),
\end{cases}
$$

and

$$
\begin{cases}
\hat{r}_m^- = -\varepsilon\sigma_2(\rho) - \frac{3}{2}\eta_1 ha_{m-1}^n - \eta_2 ha_m^n + \frac{1}{2}\eta_1 ha_{m+1}^n + \eta_1 h^2 b_{m-1}^n \\[2mm]
\qquad - \eta_1 h^2\left(\frac{h}{2}a_m^n b_{m-1}^n - \frac{1}{4}a_m^n\left(a_{m+1}^n + 3a_{m-1}^n\right)\right), \\[2mm]
\hat{r}_m^c = 2\varepsilon\sigma_2(\rho) + 2\eta_1 ha_{m-1}^n - 2\eta_1 ha_{m+1}^n + 2h^2\eta_2 b_m^n - \eta_1 h^2 a_m^n\left(a_{m+1}^n + a_{m-1}^n\right), \\[2mm]
\hat{r}_m^+ = -\varepsilon\sigma_2(\rho) - \frac{1}{2}\eta_1 ha_{m-1}^n + \eta_2 ha_m^n + \frac{3}{2}\eta_1 ha_{m+1}^n + \eta_1 h^2 b_{m+1}^n \\[2mm]
\qquad + \eta_1 h^2\left(\frac{h}{2}a_m^n b_{m+1}^n + \frac{1}{4}a_m^n\left(3a_{m+1}^n + a_{m-1}^n\right)\right), \\[2mm]
q_m^- = \eta_1 h^2\left(1 - \frac{h}{2}a_{m-1}^n\right)-, \quad q_m^c = 2\eta_2 h^2, \quad q_m^+ = \eta_1 h^2\left(1 + \frac{h}{2}a_{m+1}^n\right),
\end{cases}
$$

and H_m^n denotes the delayed term $U(x_m, t_n - s)$ which is evaluated as

$$H_m^n = \begin{cases} \phi_b(x_m, t_n), & \text{if } t_n < s, \ m = 0, 1, \ldots, N, \\ U_m^{n-s}, & \text{if } t_n \geq s, \ m = 0, 1, \ldots, N. \end{cases}$$

Also, the values for η_1 and η_2 are presented for $\eta_1 = \frac{1}{12}$ and $\eta_2 = \frac{5}{12}$.

The rearrangement of fully discrete scheme in Eq. (13) after incorporating the boundary conditions gives a linear system of the form

$$\begin{cases} \left(q_m^- + \dfrac{\Delta t}{2} r_{mn}^-\right) U_{m-1}^{n+1} + \left(q_m^c + \dfrac{\Delta t}{2} r_{mn}^c\right) U_m^{n+1} + \left(q_m^+ + \dfrac{\Delta t}{2} r_{mn}^+\right) U_{m+1}^{n+1} \\ \qquad = \left(q_m^- - \dfrac{\Delta t}{2} \hat{r}_{mn}^-\right) U_{m-1}^n + \left(q_m^c - \dfrac{\Delta t}{2} \hat{r}_{mn}^c\right) U_m^n + \left(q_m^+ - \dfrac{\Delta t}{2} \hat{r}_{mn}^+\right) U_{m+1}^n + \hat{F}_m^n, \\ U^{n+1}(0) = \phi_l(t_{n+1}), \quad U^{n+1}(1) = \phi_r(t_{n+1}), \quad 0 \leq n \leq N, \\ U^{n+1}(x) = \phi_b(x, t_{n+1}), \quad x \in \Omega_x, \quad -(s+1) \leq n \leq -1, \end{cases} \tag{19}$$

where

$$\begin{aligned} \hat{F}_m^n = & -\frac{\Delta t}{2} q_m^- \left(c_{m-1}^{n+1} H_{m-1}^{n+1} + c_{m-1}^n H_{m-1}^n\right) - \frac{\Delta t}{2} q_m^c \left(c_m^{n+1} H_m^{n+1} + c_m^n H_m^n\right) \\ & -\frac{\Delta t}{2} q_m^+ \left(c_{m+1}^{n+1} H_{m+1}^{n+1} + c_{m+1}^n H_{m+1}^n\right) + \frac{\Delta t}{2} q_m^- \left(f_{m-1}^{n+1} + f_{m-1}^n\right) \\ & +\frac{\Delta t}{2} q_m^c \left(f_m^{n+1} + f_m^n\right) + \frac{\Delta t}{2} q_m^+ \left(f_{m+1}^{n+1} + f_{m+1}^n\right). \end{aligned}$$

4 Uniform convergence analysis

The linear system developed in Eq. (19) can be put in standard matrix equation form as:

$$AV^{n+1} = BV^n + G^n, \tag{20}$$

where A and B is the tridiagonal operator defined by:

$$\begin{cases} A = \left(A_0 + \dfrac{\Delta t}{2} A_1\right), \\ B = \left(A_0 - \dfrac{\Delta t}{2} A_2\right), \end{cases} \tag{21}$$

where

$$A_0 = \begin{pmatrix} 1 & 0 & 0 & 0 & \ldots & 0 \\ q_2^- & q_2^c & q_2^+ & 0 & \ldots & 0 \\ \ldots & \ldots & \ldots & \ldots & \ldots & \ldots \\ 0 & \ldots & 0 & q_N^- & q_N^c & q_N^+ \\ 0 & \ldots & 0 & 0 & 0 & 1 \end{pmatrix}, \quad A_1 = \begin{pmatrix} 1 & 0 & 0 & 0 & \ldots & 0 \\ r_2^- & r_2^c & r_2^+ & 0 & \ldots & 0 \\ \ldots & \ldots & \ldots & \ldots & \ldots & \ldots \\ 0 & \ldots & 0 & r_N^- & r_N^c & r_N^+ \\ 0 & \ldots & 0 & 0 & 0 & 1 \end{pmatrix},$$

$$A_2 = \begin{pmatrix} 1 & 0 & 0 & 0 & \dots & 0 \\ \hat{r}_2^- & \hat{r}_2^c & \hat{r}_2^+ & 0 & \dots & 0 \\ \dots & \dots & \dots & \dots & \dots & \dots \\ 0 & \dots & 0 & \hat{r}_N^- & \hat{r}_N^c & \hat{r}_N^+ \\ 0 & \dots & 0 & 0 & 0 & 1 \end{pmatrix}, \quad V^{n+1} = \begin{pmatrix} U_1^{n+1} \\ U_2^{n+1} \\ U_3^{n+1} \\ \vdots \\ U_{N+1}^{n+1} \end{pmatrix}, \quad V^n = \begin{pmatrix} U_1^n \\ U_2^n \\ U_3^n \\ \vdots \\ U_{N+1}^n \end{pmatrix}, \quad G^n = \begin{pmatrix} \hat{F}_1^n \\ \hat{F}_2^n \\ \hat{F}_3^n \\ \vdots \\ \hat{F}_{N+1}^n \end{pmatrix}.$$

Lemma 9. *Let A be a coefficient matrix of the tridiagonal of the difference scheme in Eq. (18). Then, for all $\varepsilon > 0$, the matrix A at each temporal level is an irreducible M-matrix and so has a positive inverse.*

Proof. The difference scheme in Eq. (20) can be written in the form

$$AU^{n+1} + H_m^n + TE = 0, \tag{22}$$

where $H_m^n = -BU^n - G^n$. In Eq. (22) the related vectors are

$$TE = O\left(h^4\right), U = [U_1, U_2, \dots, U_{N+1}]^T, TE = [E_1, E_2, \dots, E_{N+1}]^T,$$

and

$$0 = [0, 0, \dots, 0]^T.$$

Let $v_m^{n+1} = \left[u_1^{n+1}, u_2^{n+1}, \dots, u_{N+1}^{n+1}\right]^T \approx U$ and $E = U^{n+1} - v^{n+1}$ be the difference between the approximate and exact solutions at level $n+1$. If we replace the exact solution with the numerical solution in Eq. (20) at the mesh points of the difference equation, we obtain an equation of the form

$$Av^{n+1} = Bv^n + G^n. \tag{23}$$

Subtracting Eq. (22) from Eq. (23), gives

$$A\left(U^{n+1} - v^{n+1}\right) = TE. \tag{24}$$

Let $\left|a_m^{n+1}\right| \le C_1$ and $\left|b_m^{n+1}\right| \le C_2$. From Eq. (20) clearly we have,

$$\left|r_m^-\right| = \left|-\varepsilon\sigma_1(\rho) - \frac{3}{2}\eta_1 hC_1 - \eta_2 hC_1 + \frac{1}{2}\eta_1 hC_1 + \eta_1 h^2 C_2\right|$$
$$+ \left|-\eta_1 h^2\left(\frac{h}{2}C_1 C_2 - \frac{1}{4}C_1(C_1 + 3C_1)\right)\right| > 0,$$

and

$$\left|r_m^+\right| = \left|-\varepsilon\sigma_1(\rho) - \frac{1}{2}\eta_1 hC_1 + \eta_2 hC_1 \frac{3}{2}\eta_1 hC_1 + \eta_1 h^2 C_2\right| +$$
$$+ \left|\eta_1 h^2\left(\frac{h}{2}C_1 C_2 + \frac{1}{4}C_1(3C_1 + C_1)\right)\right| > 0.$$

From Eq. (20), the following estimation can be obtained

$$\left|r_m^-\right| + \left|r_m^+\right| < \left|r_m^c\right|,$$

where

$$|r_m^c| = \left| 2\varepsilon \sigma_1(\rho) + 2\eta_1 h C_1 - 2\eta_1 h C_1 + 2h^2 \eta_2 C_2 - \eta_1 h^2 C_1 (C_1 + C_1) \right|.$$

Therefore, for sufficiently small h, the tridiagonal matrix A given in Eq. (20) at each temporal level is an irreducible M-matrix [20]. Thus, A is a nonsingular matrix and $A^{-1} \geq 0$. Hence, from the error Eq. (24), we have:

$$\|E\| \leq \|A^{-1}\| \|TE\|. \tag{25}$$

As a result, the difference scheme in Eq. (20) satisfies the hypotheses of Lemma 9 and immediately the required result follows. Hence, tridiagonal system in Eq. (20) can be easily solved by any existing methods. $\qquad \square$

Following the approach given in [20], let S_m be the sum of the elements of the mth row of the tridiagonal matrix A, then division of Eq. (20) by h and for sufficiently small of h we can easily obtain:

$$S_m > \frac{h^2 \eta_1}{2} C_1 C_2, \text{ because } \varepsilon \sigma(\rho) = \frac{h C_1}{2} \coth\left(\frac{C_1 \rho}{2}\right). \tag{26}$$

Let $(A)_{m,k}^{-1}$ be the $(m,k)^{th}$ element of A^{-1} and we define,

$$\|A^{-1}\| = \max_{1 \leq m \leq N+1} \sum_{k=1, m \neq k}^{N+1} (A)_{m,k}^{-1},$$

and

$$\|TE\| = \max_{1 \leq m \leq N+1} |TE_m|. \tag{27}$$

Since $A^{-1} \geq 0$, from the theory of matrices, we have $\sum_{k=1, m \neq k}^{N+1} (A)_{m,k}^{-1} S_k = 1$ for $1 \leq m \leq N+1$. This becomes

$$\sum_{k=1, m \neq k}^{N-1} (A)_{m,k}^{-1} \leq \frac{1}{\min_{1 \leq m \leq N+1} S_k} \leq \frac{2}{h^2 \eta_1 C_1 C_2}. \tag{28}$$

From Eqs. (26)-(28), we get:

$$\|E\| \leq \frac{2}{h^2 \eta_1 C_1 C_2} \times O\left(h^4\right) \leq Ch^2. \tag{29}$$

In Eq. (29), the value of C is independent of mesh size h. This shows, the spatial discretization process is uniformly convergent of second order. From Lemma 7 and Eq. (29) it is observed that $\|E\| \to 0$ as $\Delta t \to 0$ and $h \to 0$, which proves the consistency of the method. Using Lemma 7 and Eq. (29), and the Lax equivalence theorem (see [10]), we have the following main result .

Theorem 1 (**Error in the fully discrete scheme**). *Let u be the solution of the problem in Eqs. (1)-(3) and U be the approximation solution of fully discretized scheme obtained from the scheme in Eq. (19). Then, we have the following parameter-uniform error estimation*

$$\|u - U\| \leq C\left((\Delta t)^2 + h^2\right),$$

where $C > 0$ is a constant and independent of ε.

5   Numerical experiments

To estimate the ε-uniform convergence of the proposed method, we use the double mesh principle as the exact solution of the problems are not known. The maximum pointwise errors $E_\varepsilon^{N,\Delta t}$ and the corresponding order of convergence $p_\varepsilon^{N,\Delta t}$ are computed as

$$E_\varepsilon^{N,\Delta t} = \max_{m,n} \left| U_{m,n}^{N,\Delta t} - U_{m,n}^{4N,\frac{\Delta t}{2}} \right|, \quad p_\varepsilon^{N,\Delta t} = \log_2 \left(\frac{E_\varepsilon^{N,\Delta t}}{E_\varepsilon^{4N,\frac{\Delta t}{2}}} \right),$$

and from these values we obtain the ε-uniform error $E^{N,\Delta t}$ and the corresponding ε-uniform order of convergence $p^{N,\Delta t}$ by

$$E^{N,\Delta t} = \max_\varepsilon E_\varepsilon^{N,\Delta t} \text{ and } p^{N,\Delta t} = \log_2 \left(\frac{E^{N,\Delta t}}{E^{4N,\frac{\Delta t}{2}}} \right),$$

where $U_{m,n}^{N,\Delta t}$ is the numerical solutions obtained by using N and M mesh intervals in space and time direction, respectively. To compute $U_{m,n}^{4N,\frac{\Delta t}{2}}$ we use $4N$ and $2M$ mesh intervals in spatial and temporal direction, respectively.

Example 1. Consider the following singularly perturbed delay parabolic initial boundary value problem:

$$\begin{cases} \dfrac{\partial u}{\partial t} - \varepsilon \dfrac{\partial^2 u}{\partial x^2} + (2 - x^2) \dfrac{\partial u}{\partial x} + (x+1)(t+1)u(x,t) = -u(x, t - \tau) + 10t^2 \exp(-t)x(1-x), \\ (x,t) \in D = (0,1) \times [0,2], \\ u(x,t) = 0, (x,t) \in [0,1] \times [-1,0], \\ u(0,t) = 0, u(1,t) = 0, t \in [0,2]. \end{cases}$$

Example 2. Consider the following singularly perturbed delay parabolic initial boundary value problem:

$$\begin{cases} \dfrac{\partial u}{\partial t} - \varepsilon \dfrac{\partial^2 u}{\partial x^2} + (2 - x^2) \dfrac{\partial u}{\partial x} + xu(x,t) = -u(x, t - \tau) + 10t^2 \exp(-t)x(1-x), \\ (x,t) \in D = (0,1) \times [0,2], \\ u(x,t) = 0, (x,t) \in [0,1] \times [-1,0], \\ u(0,t) = 0, u(1,t) = 0, t \in [0,2]. \end{cases}$$

The results tabulated for $U_{m,n}^{4N,\frac{\Delta t}{2}}$ in Table 1 and Table 3 are obtained by taking $4N$ and $2M$ mesh intervals for various values of ε, to confirm that the numerical methods presented in this paper are second order ε-uniform convergent. Also, we can observe the ε - uniform convergence of the present method from Table 2 and Table 4 as maximum point wise errors decrease when the numerical rates of convergence increase as the number of mesh points in the spatial direction and temporal directions increases. Graphs of the numerical solution of Example 1 for $\varepsilon = 1, \varepsilon = 2^{-16}$ and $N = 32, \Delta t = 0.1/4$ are plotted in Figure 1. The two figures (Figure 1a and Figure 1b) also shows to visualize the appearance of boundary layers in the solutions and to show the effect of the parameter ε on the boundary layer. We have plotted the present numerical results of maximum pointwise errors in log-log scale for Example 1 in Figure 2a and for Example 2 in Figure 2b. These graphs demonstrate the robustness and effectiveness of

Table 1: Maximum pointwise errors $E_\varepsilon^{N,\Delta t}$ and rate of convergence $p_\varepsilon^{N,\Delta t}$ for Example 1.

$\varepsilon\downarrow$	$N=8$	$N=32$	$N=128$	$N=512$
	$M=16$	$M=32$	$M=64$	$M=128$
2^{-10}	1.0147e-02	3.1183e-03	6.3516e-04	1.0991e-04
	1.7022	2.2956	2.5308	–
2^{-12}	1.0147e-02	3.1183e-03	6.4733e-04	1.4305e-04
	1.7022	2.2682	2.1780	–
2^{-14}	1.0147e-02	3.1183e-03	6.4733e-04	1.4315e-04
	1.7022	2.2682	2.1770	–
2^{-16}	1.0147e-02	3.1183e-03	6.4733e-04	1.4315e-04
	1.7022	2.2682	2.1770	–
2^{-18}	1.0147e-02	3.1183e-03	6.4733e-04	1.4315e-04
	1.7022	2.2682	2.1770	–
2^{-20}	1.0147e-02	3.1183e-03	6.4733e-04	1.4315e-04
	1.7022	2.2682	2.1770	–
2^{-22}	1.0147e-02	3.1183e-03	6.4733e-04	1.4315e-04
	1.7022	2.2682	2.1770	–
2^{-24}	1.0147e-02	3.1183e-03	6.4733e-04	1.4315e-04
	1.7022	2.2682	2.1770	–
2^{-28}	1.0147e-02	3.1183e-03	6.4733e-04	1.4315e-04
	1.7022	2.2682	2.1770	–
2^{-30}	1.0147e-02	3.1183e-03	6.4733e-04	1.4315e-04
	1.7022	2.2682	2.1770	–
$E^{N,\Delta t}$	**1.0147e-02**	**3.1183e-03**	**6.4733e-04**	**1.4315e-04**
$p^{N,\Delta t}$	**1.7022**	**2.2682**	**2.1770**	**-**

Table 2: Maximum pointwise errors $E_\varepsilon^{N,\Delta t}$ of the scheme for Example 1.

$\varepsilon\downarrow$	$N=32$	$N=64$	$N=128$	$N=256$	$N=512$
	$M=40$	$M=80$	$M=160$	$M=320$	$M=640$
2^{-0}	9.9905e-05	5.2752e-05	2.7153e-05	1.3781e-05	6.9431e-06
2^{-2}	3.4237e-04	1.6887e-04	8.4058e-05	4.1969e-05	2.0972e-05
2^{-4}	7.6614e-04	3.0469e-04	1.3282e-04	6.1592e-05	2.9610e-05
2^{-6}	1.9935e-03	6.5790e-04	2.2595e-04	8.6204e-05	3.6485e-05
2^{-8}	3.2243e-03	1.4593e-03	5.2502e-04	1.7066e-04	5.8113e-05
2^{-10}	3.2592e-03	1.6859e-03	8.4262e-04	3.7136e-04	1.3271e-04
2^{-12}	3.2592e-03	1.6861e-03	8.5478e-04	4.2992e-04	2.1239e-04
2^{-14}	3.2592e-03	1.6861e-03	8.5478e-04	4.2999e-04	2.1560e-04
2^{-16}	3.2592e-03	1.6861e-03	8.5478e-04	4.2999e-04	2.1560e-04
2^{-18}	3.2592e-03	1.6861e-03	8.5478e-04	4.2999e-04	2.1560e-04
2^{-20}	3.2592e-03	1.6861e-03	8.5478e-04	4.2999e-04	2.1560e-04
2^{-24}	3.2592e-03	1.6861e-03	8.5478e-04	4.2999e-04	2.1560e-04
2^{-28}	3.2592e-03	1.6861e-03	8.5478e-04	4.2999e-04	2.1560e-04
2^{-30}	3.2592e-03	1.6861e-03	8.5478e-04	4.2999e-04	2.1560e-04
$E^{N,\Delta t}$	**3.2592e-03**	**1.6861e-03**	**8.5478e-04**	**4.2999e-04**	**2.1560e-04**
$p^{N,\Delta t}$	**0.95083**	**0.98007**	**0.99125**	**0.99595**	**-**

Table 3: Maximum pointwise errors $E_\varepsilon^{N,\Delta t}$ and rate of convergence $p_\varepsilon^{N,\Delta t}$ for Example 2.

$\varepsilon\downarrow$	$N = 8$ $M = 16$	$N = 32$ $M = 32$	$N = 128$ $M = 64$	$N = 512$ $M = 128$
2^{-10}	1.9564e-02	7.2307e-03	1.9667e-03	2.5977e-04
	1.4360	1.8784	2.9205	–
2^{-12}	1.9564e-02	7.2307e-03	2.0043e-03	5.0486e-04
	1.4360	1.8510	1.9891	–
2^{-14}	1.9564e-02	7.2307e-03	2.0043e-03	5.1486e-04
	1.4130	1.8465	1.9608	–
2^{-16}	1.9564e-02	7.2307e-03	2.0043e-03	5.1486e-04
	1.4130	1.8465	1.9608	–
2^{-18}	1.9564e-02	7.2307e-03	2.0043e-03	5.1486e-04
	1.4130	1.8465	1.9608	–
2^{-20}	1.9564e-02	7.2307e-03	2.0043e-03	5.1486e-04
	1.4130	1.8465	1.9608	–
2^{-22}	1.9564e-02	7.2307e-03	2.0043e-03	5.1486e-04
	1.4130	1.8465	1.9608	–
2^{-24}	1.9564e-02	7.2307e-03	2.0043e-03	5.1486e-04
	1.4130	1.8465	1.9608	–
2^{-28}	1.9564e-02	7.2307e-03	2.0043e-03	5.1486e-04
	1.4130	1.8465	1.9608	–
2^{-30}	1.9564e-02	7.2307e-03	2.0043e-03	5.1486e-04
	1.4130	1.8465	1.9608	–
$E^{N,\Delta t}$	**1.9564e-02**	**7.2307e-03**	**2.0043e-03**	**5.1486e-04**
$p^{N,\Delta t}$	**1.4130**	**1.8465**	**1.9608**	-

Table 4: Maximum pointwise errors $E_\varepsilon^{N,\Delta t}$ of the scheme for Example 2.

$\varepsilon\downarrow$	Number of mesh intervals $N = M$				
	32	64	128	256	512
2^{-0}	1.0749e-04	5.8531e-05	3.0614e-05	1.5660e-05	7.9207e-06
2^{-2}	5.4983e-04	2.9405e-04	1.5246e-04	7.7670e-05	3.9206e-05
2^{-4}	1.1863e-03	5.3173e-04	2.6476e-04	1.3288e-04	6.6635e-05
2^{-6}	3.3040e-03	1.1073e-03	4.1432e-04	1.7826e-04	8.4960e-05
2^{-8}	7.1097e-03	3.0887e-03	9.6542e-04	3.1847e-04	1.1859e-04
2^{-10}	7.2307e-03	3.8516e-03	1.9512e-03	8.0308e-04	2.5301e-04
2^{-12}	7.2307e-03	3.8523e-03	1.9892e-03	1.0105e-03	4.9936e-04
2^{-14}	7.2307e-03	3.8523e-03	1.9892e-03	1.0107e-03	5.0944e-04
2^{-16}	7.2307e-03	3.8523e-03	1.9892e-03	1.0107e-03	5.0944e-04
2^{-18}	7.2307e-03	3.8523e-03	1.9892e-03	1.0107e-03	5.0944e-04
2^{-20}	7.2307e-03	3.8523e-03	1.9892e-03	1.0107e-03	5.0944e-04
2^{-24}	7.2307e-03	3.8523e-03	1.9892e-03	1.0107e-03	5.0944e-04
2^{-28}	7.2307e-03	3.8523e-03	1.9892e-03	1.0107e-03	5.0944e-04
2^{-30}	7.2307e-03	3.8523e-03	1.9892e-03	1.0107e-03	5.0944e-04
$E^{N,\Delta t}$	**7.2307e-03**	**3.8523e-03**	**1.9892e-03**	**1.0107e-03**	**5.0944e-04**
$p^{N,\Delta t}$	**0.90842**	**0.95353**	**0.97683**	**0.98837**	-

Table 5: Comparison of uniform error ($E^{N,\Delta t}$) and uniform rate of convergence ($p^{N,\Delta t}$) for Example 1.

Methods		$N = 32$	$N = 64$	$N = 128$	$N = 256$
		$M = 40$	$M = 80$	$M = 160$	$M = 320$
Proposed method	$E^{N,\Delta t}$	3.2592e-03	1.6861e-03	8.5478e-04	4.2999e-04
	$p^{N,\Delta t}$	0.95083	0.98007	0.99125	-
Method in, [16]	$E^{N,\Delta t}$	7.8114e-03	4.1163e-03	2.1158e-03	1.0729e-03
	$p^{N,\Delta t}$	0.9242	0.9601	0.9797	-
Method in, [4]	$E^{N,\Delta t}$	9.2390e-3	5.4553e-3	3.1384e-3	1.7623e-3
	$p^{N,\Delta t}$	0.7601	0.7976	0.8325	0.8598
Method in, [7]	$E^{N,\Delta t}$	9.9504e-03	5.8541e-03	3.3439e-03	1.8650e-03
	$p^{N,\Delta t}$	0.7653	0.8079	0.8424	-
		$N = M = 32$	$N = 64$	$N = 128$	$N = 256$
Proposed method	$E^{N,\Delta t}$	3.1183e-03	1.6167e-03	8.2040e-04	4.1290e-04
	$p^{N,\Delta t}$	0.94771	0.97865	0.99054	-
Method in, [9]	$E^{N,\Delta t}$	1.72e-02	9.00e-03	4.58E-03	2.30e-03
	$p^{N,\Delta t}$	0.9344	0.9746	0.9937	-

Table 6: Comparison of uniform error ($E^{N,\Delta t}$) and uniform rate of convergence ($p^{N,\Delta t}$) for Example 2.

Methods		$N = M = 32$	$N = 64$	$N = 128$	$N = 256$
Proposed method	$E^{N,\Delta t}$	7.2307e-03	3.8523e-03	1.9892e-03	1.0107e-03
	$p^{N,\Delta t}$	0.90842	0.95353	0.97683	-
Method in, [9]	$E^{N,\Delta t}$	1.84e-02	9.38e-03	4.67e-03	2.31e-03
	$p^{N,\Delta t}$	0.9720	1.0062	1.0155	-

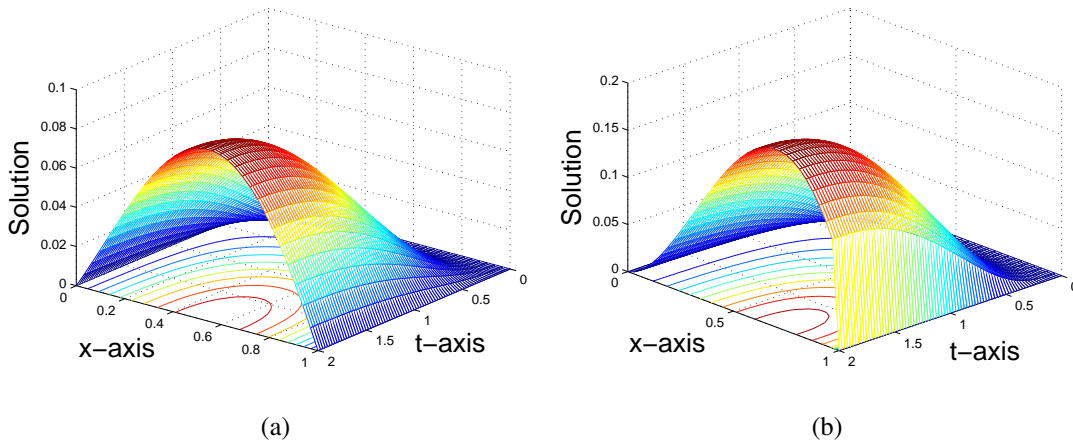(a)   (b)

Figure 1: Numerical solution for Example 1 for different values of ε and T **(a)** $\varepsilon = 1$, **(b)** $\varepsilon = 2^{-16}$.
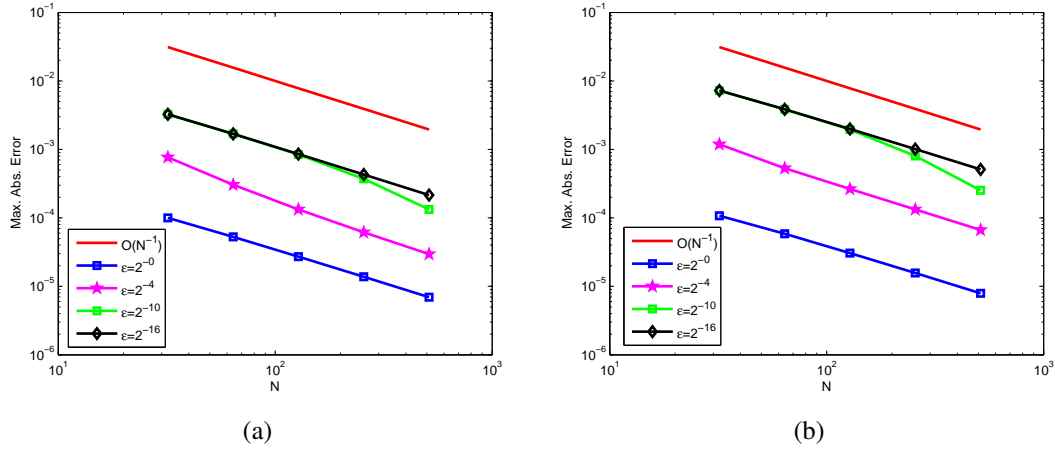
Figure 2: Example 1 on left and Example 2 on right, Log-Log plot between N and maximum absolute error.

the numerical approach developed in this paper. In Table 5 and Table 6 we are comparing the maximum absolute errors and rate of convergence obtained by the proposed method for the problems in Example 1 and Example 2 respectively. The two tables (Table 5 and Table 6) also clearly indicate that the errors of exponentially fitted finite difference scheme presented in this paper are much smaller than those obtained using a boundary-layer resolving method. From these tables we can confirm the improved accuracy of our proposed numerical method. It should be noted that the MATLAB R2013A program was used to execute the computations connected to the illustrations of each Example in this work.

6 Conclusion

An efficient numerical method based on the exponentially fitted method has been proposed for solving a class of one-dimensional singularly perturbed large time delay parabolic partial differential equations of convection-diffusion type that arise in the automatically controlled furnace model. We have proved that the method provides second-order accurate ε-uniform convergent in both time and space. The approach can also be used to solve equations with delays, which might be constant, time-dependent, or random. As $\varepsilon \to 0$, the suggested method may be applied to singularly perturbed parabolic reaction-diffusion problems exhibit boundary layers in the neighborhood of both along $x = 0$ and $x = 1$. However, the solutions in this situation have a different type of layer than the layers discussed in this article. The performance of the proposed approach is investigated by evaluating with most of the current methods. From the numerical experiments, it is observed that, the more efficiency and high accuracy of this method. An interesting feature of this method is that, it is not necessary to impose any restriction on mesh formation. On the basis of the numerical results of the two examples, it is concluded that the present method offers significant advantage for the singularly perturbed delay parabolic partial differential equations of convection diffusion type with large time lag.

Acknowledgements

References

[1] A. Ansari, S. Bakr, G. Shishkin, *A parameter-robust finite difference method for singularly perturbed delay parabolic partial differential equations*, J. Comput. Appl. Math. **205** (2007) 552–566.

[2] I.T. Daba, G.F. Duressa, *Extended cubic B-spline collocation method for singularly perturbed parabolic differential-difference equation arising in computational neuro science*, Internat. J. Numer. Methods Engrg. **37** (2021) e3418.

[3] A. Das, S. Natesan, *Uniformly convergent hybrid numerical scheme for singularly perturbed delay parabolic convection-diffusion problems on Shishkin mesh*, Appl. Math. Comput. **271** (2015) 168–186.

[4] A. Das, S. Natesan, *Second-order uniformly convergent numerical method for singularly perturbed delay parabolic partial differential equations*, Int. J. Comput. Math. **95** (2018) 490–510.

[5] G.F. Duressa, H.G. Debela, *Numerical solution of singularly perturbed differential difference equations with mixed parameters*, J. Math. Model. (2021) 1–15.

[6] I.R. Epstein, *Delay effects and differential delay equations in chemical kinetics*, Int. Rev. Phys. Chem. **11** (1992) 135–160.

[7] S. Gowrisankar, S. Natesan, *ε-uniformly convergent numerical scheme for singularly perturbed delay parabolic partial differential equations*, Int. J. Comput. Math. **94** (2017) 902–921.

[8] M.J. Kabeto, G.F. Duressa, *Robust numerical method for singularly perturbed semilinear parabolic differential difference equations*, Math. Comput. Simul. **188** (2021) 537–547.

[9] D. Kumar, P. Kumari, *A parameter-uniform numerical scheme for the parabolic singularly perturbed initial boundary value problems with large time delay*, J. Appl. Math. Comput. **59** (2019) 179–206.

[10] J. Miller, E. O'Riordan, G. Shishkin, R.B. Kellogg, *Fitted numerical methods for singular perturbation problems*, SIAM Rev. **39** (1997) 535–537.

[11] F. Mirzaee, K. Sayevand, S. Rezaei, *Finite difference and spline approximation for solving fractional stochastic advection-diffusion equation*, Iran J. Sci. Technol. Trans. A Sci. **45** (2021) 607–617.

[12] F. Mirzaee, S. Bimesl, E. Tohidi, *A numerical framework for solving high-order pantograph-delay Volterra integro-differential equations*, Kuwait J. Sci. **43** (2016) 1.

[13] F. Mirzaee, S. Bimesl, *A uniformly convergent euler matrix method for telegraph equations having constant coefficients*, Mediterr. J. Math. **13** (2016) 497–515.

[14] F. Mirzaee, S.F. Hoseini, *Solving singularly perturbed differential-difference equations arising in science and engineering with Fibonacci polynomials*, Results Phys. **3** (2013) 134–141.

[15] R.E. O'Malley, *Introduction to Singular Perturbations*, Academic Press, 1974.

[16] P.C. Podila, K. Kumar, *A new stable finite difference scheme and its convergence for time-delayed singularly perturbed parabolic pdes*, J. Comput. Appl. Math. **39** (2020) 1–16.

[17] D.L. Scharfetter, H.K. Gummel, *Large-signal analysis of a silicon read diode oscillator*, IEEE Trans. Electron Devices **16** (1969) 64–77.

[18] R.M. Symko, L. Glass, *Spatial switching in chemical reactions with heterogeneous catalysts*, J. Chem. Phys. **60** (1974) 835–841.

[19] A.V. Harten, J. Schumacher, *On a class of partial functional differential equations arising in feedback control theory*, North-Holland Math. Stud. **31** (1978) 161–179.

[20] J.M. Varah, *A lower bound for the smallest singular value of a matrix*, Linear Algebra Appl. **11** (1975) 3–5.

[21] M.M. Woldaregay, G.F. Duressa, *Robust mid-point upwind scheme for singularly perturbed delay differential equations*. Comp. Appl. Math. **40** (2021) 178.

[22] J. Wu, *Theory and Applications of Partial Functional Differential Equations*, Springer Sci. Business Media, 2012.